Estimates of the coherent leakage of sound from an ocean surface duct

Adrian D. Jones[1], Alec J. Duncan[2], Zhi Yong Zhang[1]

[1]Defence Science and Technology Group, P.O. Box 1500, Edinburgh, SA 5111, Australia
[2]Centre for Marine Science & Technology, Curtin University, GPO Box U1987, Perth WA 6845, Australia

ABSTRACT

For underwater sound transmission in a mixed-layer surface duct, the trapping of sound and the coherent leakage of some of this energy from the duct are well known phenomena. Models of sound transmission which include wave effects, such as modal models or Parabolic Equation models, include implicit determinations of the rates of coherent leakage. However for some applications it is useful or instructive to obtain direct analytic determinations of the leakage. Work carried out by the authors on the derivation of an approximate algorithm for the rate of coherent duct leakage is presented, along with comparisons with leakage rates determined by a wave-type model for several surface duct scenarios.

1. INTRODUCTION

In a deep ocean, sound may travel within the mixed layer surface duct with much less Transmission Loss (*TL*) to long ranges than at other depths. As is well known, the duct is formed as the motion of the sea surface mixes the water to a particular depth. The resulting near-uniform temperature causes a rise in sound speed with depth at a rate of about 0.016 s^{-1}, down to the thermocline in which the temperature and sound speed decline with depth. Sound travelling near the surface within a small span of angles about the horizontal is constrained by refraction at the lower duct boundary, and by reflection at the ocean surface, to remain in the mixed layer duct.

Sound travelling within the surface duct will be subject to a spreading loss, but beyond a short range from the source, the spreading will be approximately cylindrical. Other losses to transmission will occur if sound impinging on a rough sea surface is scattered to angles too great to be constrained within the duct, and if the process of refraction at the lower duct boundary does not return all sound energy to the duct. The latter phenomenon is the leakage of sound which is considered in this paper.

The authors considered the issue of leakage from the surface duct in earlier work (Jones et al, 2015, 2016) and so this paper presents the latest findings in this investigation. The present paper includes a brief summary of the earlier work, but the reader is referred to the earlier paper (Jones et al., 2015) for more details, including descriptions of prior work in the literature.

2. SUMMARY OF DUCT LEAKGAGE EFFECT AND DESCRIPTIONS

As is well-known, "duct leakage" is a coherent effect, whereas the loss from surface scattering is an incoherent effect. Also, duct leakage may be considered as a modal effect, with the rate of leakage for each mode, in units of dB/km, being uniform with range. The leakage rate is lower for each mode of lower mode number *m*. The rate of leakage from modes of number $m = 2$ and higher may be shown to be quite large relative to the leakage of the first mode, for each given frequency, and so for practical applications it is necessary to consider the leakage rate of the first mode, only. The parameters determining the rate of leakage from the surface duct are: the sound speed gradient in the duct g in units s^{-1}, the sound speed gradient below the duct g_t, the duct thickness D metres, acoustic frequency *f* Hz and speed of sound at the ocean surface c_w m/s. Following from the work of Furry (Kerr, 1951), Marsh (1950) and Pederson and Gordon (1965, 1970), a relevant parameter is the ratio of sound speed gradients $\rho = (g/g_t)^{1/3}$, where ρ is negative.

2.1 Trapping within surface duct

For sound travelling near to horizontal, the phenomenon of duct trapping may be considered to result from the in-phase reinforcement of sound reflected downward from the ocean surface with sound refracted upward from the region of the lower duct boundary. An approximate expression for the lowest frequency, $f_{c,m}$ Hz, for which this reinforcement may occur for mode number $m = 1, 2, 3...$, may be shown to be

$$f_{c,m} \approx \frac{1}{2\pi\sqrt{2g}}\left(\frac{-a_m c_w}{D}\right)^{3/2} \tag{1}$$

where the values a_m are the mth zeros of $\mathrm{Ai}(a)$, the Airy function. Numerical determinations (e.g. Miller (1946), table III) give $a_1 = -2.338107$, $a_2 = -4.087949$, $a_3 = -5.520560$, etc. Using the well-known approximation $a_m \approx -\left[3\pi\left(m-\tfrac{1}{4}\right)/2\right]^{2/3}$, the more familiar expression is obtained as

$$f_{c,m} \approx \frac{3\left(m-1/4\right)}{4\sqrt{2g}}\left(\frac{c_w}{D}\right)^{3/2}. \tag{2}$$

Equation (2) corresponds with a ray-based description of the sound path, where the path is presumed to be described by a limiting ray in the duct, and a phase change (advance) of $\pi/2$ is included to account for the caustic at the ray turning point (see, e.g. Medwin and Clay (1998) page 96). For values of the gradient ratio ρ typical of real oceans, the rate of duct leakage varies continuously as frequency changes from below $f_{c,m}$ Hz to above $f_{c,m}$ Hz.

For convenience, a dimensionless parameter *M* is introduced, this describing the surface duct "strength":

$$M = \left(2k^2 g/c_w\right)^{1/3} D = 2D\left[\pi^2 f^2 g\right]^{1/3}/c_w \tag{3}$$

where $k = 2\pi f/c_w$ is acoustic wave number, m^{-1}. Substituting using Equation (1) gives the value of *M* for cut-on of mode *m* as $M_m \approx -a_m$, and for example $M_1 \approx 2.3381$ and $M_2 \approx 4.0879$.

2.2 Determination of leakage rates

As is well known, the attenuation rate for sound pressure amplitude for mode *m*, in nepers/m, is equal to the imaginary part of the horizontal wave number of the mode, $\mathrm{Im}(\lambda_m)$, so the intensity loss becomes

$$A_m = -1000 \times 20\left[\log_{10}(e)\right]\mathrm{Im}(\lambda_m) \approx -8686\,\mathrm{Im}(\lambda_m) \text{ dB/km} \tag{4}$$

where λ_m is the horizontal wave number, and is given by (e.g. Equation (10) of Pederson and Gordon (1965))

$$\lambda_m = \left[k^2 - Mx_m\left(M/D\right)^2\right]^{1/2} \tag{5}$$

where Mx_m is a root of a characteristic equation involving Hankel functions.

The wave number term *k* dominates Equation (5) and a suitable approximation for $\mathrm{Im}(\lambda_m)$ becomes

$$\mathrm{Im}(\lambda_m) \approx -\left(\left[\pi f g^2\right]^{1/3}/c_w\right)\mathrm{Im}(Mx_m). \tag{6}$$

A solution for the leakage rate in dB/km then follows from this expression for the imaginary part of the horizontal wave number using the imaginary component of Mx_m. Furry (Kerr, 1951) derived asymptotic approximations, by which $\mathrm{Im}(Mx_m)$ might be determined so long as convergence occurs.

2.2.1 Frequencies above mode cut-on

From Furry's Equation (548), which is a suitable approximation when ρ is negative and *M* large:

$$\mathrm{Im}(Mx_m) \approx \tfrac{1}{4}\alpha_m\left(\exp\left[-\tfrac{4}{3}\left(1-\rho^3\right)\left|M-\left|\zeta_m\right|\right|^{3/2}\right]\right)\left[1+\tfrac{1}{24}\left(1-\rho^{-3}\right)\left|M-\left|\zeta_m\right|\right|^{-3/2}+\ldots\right] \tag{7}$$

where $m = 1, 2, 3...$ is mode number, ς_m are solutions of the Hankel function $h_2(\varsigma_m) = 0$ and it may be shown that $|\varsigma_1| \approx 2.3381$, $|\varsigma_2| \approx 4.0879$, etc. (e.g. Kerr (1951) page 95), and also $|\varsigma_m| = -a_m$ used above. Also $\alpha_m = -\mathrm{Bi}(-|\varsigma_m|)/\mathrm{Ai}'(-|\varsigma_m|)$ where $\mathrm{Ai}(x)$ and $\mathrm{Bi}(x)$ are Airy functions, and (e.g. Furry (Kerr, 1951) page 151) $\alpha_1 \approx 0.6474$, $\alpha_2 \approx 0.4935$, $\alpha_1 \approx 0.4252$, with $\alpha_m \approx \left[\frac{3}{2}(m - \frac{1}{4})\pi\right]^{-1/3}$ an approximation.

If *M* is sufficiently large and ρ is not too small, the term in square brackets may be eliminated and, for the first mode, Equation (7) becomes $\mathrm{Im}(Mx_1) \approx \frac{1}{4}\alpha_1 \exp\left(-\frac{4}{3}(1-\rho^3)(M - |\varsigma_1|)^{3/2}\right)$. The attenuation rate $A_1(f)$ is then

$$A_1(f) \approx \frac{1406}{c_w}\left(\left[\pi f g^2\right]^{1/3}\right)\exp\left[-\tfrac{4}{3}(1-g/g_t)(M-2.3381)^{3/2}\right]\mathrm{dB/km} \tag{8}$$

where $|\varsigma_1|$ has been replaced by its numeric value, $1-g/g_t$ has replaced $1-\rho^3$, and since the sound speed gradient in the thermocline g_t is negative, the term $-g/g_t$ is positive. Note also that since $M \approx 2.3381$ for cut-on of the first mode, and as Equation (8) is used only for frequencies above cut-on, the term $(M-2.3381)$ has plain brackets in place of the modulus as it is always positive. From Equation (8) it follows that the attenuation rapidly reduces as frequency rises, due to the term in *M* in the exponent. The attenuation also decreases as the magnitude of the gradient in the thermocline, $|g_t|$, decreases. At a first level approximation, Equation (8) may be used so long as the higher order terms indicated in Equation (7) may be neglected.

An equivalent form of Equation (8) in terms of frequency *f*, where frequency $f > f_{c,1}$, is

$$A_1(f) \approx \frac{8686 \times \frac{1}{4}\alpha_1}{c_w}\left(\left[\pi f g^2\right]^{1/3}\right)\exp\left[-\tfrac{4}{3}(1-g/g_t)|\varsigma_1|^{3/2}\left(\left(\frac{f}{f_{c,1}}\right)^{2/3} - 1\right)^{3/2}\right]\mathrm{dB/km}\,. \tag{9}$$

2.2.2 Frequencies below mode cut-on

Furry's Equation (541) is a suitable approximation for $-M/\rho$ small. Considering imaginary parts, it follows that:

$$\mathrm{Im}(Mx_m) \approx \frac{[\mathrm{Im}(\varsigma_m)]}{\rho^2}\left[1 - \frac{(1-\rho^3)}{90}\left(\frac{M}{\rho}\right)^6 + \frac{(1-\rho^3)}{1260}\left(\frac{M}{\rho}\right)^8 \mathrm{Im}[(\varsigma_m)] + ...\right] \tag{10}$$

where $\varsigma_m = |\varsigma_m| e^{2\pi i/3}$ and hence $\mathrm{Im}(\varsigma_m) = 0.8660|\varsigma_m|$, giving e.g. $\mathrm{Im}(\varsigma_1) = 2.0249$. If $-M/\rho$ is small, all higher order terms shown in the square brackets are negligible, and $\mathrm{Im}(Mx_m) \approx \mathrm{Im}(\varsigma_m)/\rho^2$. For mode $m = 1$, $\mathrm{Im}(Mx_1) \approx 2.0249/\rho^2$ and the attenuation rate $A_1(f)$ is

$$A_1(f) \approx \frac{8686\,\mathrm{Im}(\varsigma_1)}{\rho^2 c_w}\left(\left[\pi f g^2\right]^{1/3}\right) \approx \frac{17.6 \times 10^3}{\rho^2 c_w}\left[\pi f g^2\right]^{1/3}\ \mathrm{dB/km} = \frac{17.6 \times 10^3}{c_w}\left[\pi f g_t^{\,2}\right]^{1/3}\ \mathrm{dB/km}\,. \tag{11}$$

2.2.3 Leakage of total signal

As the leakage rate for the first mode is much less than the leakage rates for the second and higher modes, the attenuation rates for the total signal may be estimated using Equations (8) or (9), and(11), so long as the value of *M* is appropriate for an acceptable error. In practice, this has the result that these expressions may not be used for frequencies close to the duct trapping frequency $f_{c,1}$, with the allowable proximity to $f_{c,1}$ decreasing as the below layer gradient g_t becomes large in amplitude.

3. SIMULATIONS OF TRANSMISSION IN SURFACE DUCT

A number of simulations of sound transmission within a surface duct were made using wave-type models known to describe the relevant physics responsible for duct leakage. These simulations were interrogated so that the rate of leakage of sound from the surface duct might be determined for a range of frequency values from below that for trapping of the first mode, to that for which at least two modes were expected to be trapped. The simulations are described in detail by Jones et al. (2015). The leakage rate data shown in this paper were obtained using the normal mode model ORCA (Westwood et al., 1996). Here, the leakage rate for the first mode was found directly from the model's complex mode finder. These leakage values were compared to expressions of section 2.

The scenario was for a sound source at 7 m depth in a surface duct of 50 m over a thermocline typical of a deep ocean. The sound speed gradient in the surface duct was $g = 0.016\,\mathrm{s}^{-1}$, the gradient in the 25 m layer immediately below the duct was $g_t = -0.1512\,\mathrm{s}^{-1}$ and sound speed at the surface $c_w = 1539.7483\,\mathrm{m/s}$. The entire thermocline is not uniform, but the latter value of gradient below the duct will be presumed, with the value $\rho = (g/g_t)^{1/3} = -0.473$. ORCA runs included Thorp absorption (e.g. Urick (1983) page 108), with the ORCA code incorporating the expression

$$a_V = 0.1F^2/(1+F^2) + 40F^2/(4100+F^2) + 2.75\times10^{-4}F^2 \ \ \mathrm{dB/kyd} \tag{12}$$

where *F* is frequency in kHz. This is converted to dB/km by multiplying by 1.09361.

Values of leakage rate cited in this paper have had the Thorp attenuation described by Equation (12) removed unless indicated. From Equation (1), the duct trapping frequency for the first mode $f_{c,1}$ follows as 543.6 Hz. Likewise the trapping frequency for the second mode is $f_{c,1} = 1{,}256.7$ Hz.

3.1 Comparison with theoretical rates of leakage from duct

The attenuation rate at frequencies above duct trapping may be estimated using Equation (8), so long as the higher order term in Equation (7) may be neglected. As a rough approximation, it may be assumed that if the values of *M* and ρ are such that the higher order term in the square brackets in Equation (7) has a value of 0.5 or larger, then Equation (8) will be increasingly erroneous at progressively lower frequencies. The allowable values of *M* are then presumed to be $M \geq 2.3381 + \left(\left[1 - g_t/g\right]/12\right)^{2/3}$. From Equation (3), this lower limiting value of *M* implies a lower limiting value of frequency *f*. Similarly, for frequencies below the duct trapping frequency, allowable values of *M* may be presumed to be $M \leq 1.886\left|g/g_t\right|^{1/3}/\left(1-g/g_t\right)^{1/6}$ so that the first higher order term in Equation (10) is less than 0.5. For the test scenario, it follows that Equations (8) and (11) with no higher order terms are presumed adequate for $M \geq 3.25$ and $M \leq 0.88$, that is for frequencies ≥ 891 Hz and ≤ 125 Hz, respectively.

Leakage rates for the 1st mode in the surface duct, as determined using versions of Equations (8) and (11) which do incorporate the respective first higher order terms, are shown in Figure 1 by the red dashed line and green dashed line, respectively, for frequency ranges both within and beyond those for which they are relevant. The leakage rates determined using Equations (8) and (11) "as is", without any higher order terms, are shown in the figure by the continuous red and green lines. These leakage rates are compared with those obtained numerically using ORCA, inclusive of Thorp absorption, in magenta, and with Thorp absorption subtracted, in yellow. Further, values of leakage determined using the formulation of Packman (1990) are shown in the figure as the dark blue line. These calculations used Packman's algorithm as it is shown by Ainslie (2010), with one exception – the duct trapping frequency was determined using the actual sound speed and sound speed gradient values for the duct rather than using pre-determined values. The Thorp absorption rate is shown separately as the light blue line. Clearly, for the surface duct of depth 50 m, the leakage rate of the 1st mode is less than the in-water absorption at frequencies greater than about 1100 Hz, and at progressively higher frequencies the issue of modal leakage is irrelevant.

The leakage rates determined by Equation (8), for frequencies for which $M \geq 2.3381 + \left(\left[1 - g_t/g\right]/12\right)^{2/3}$, that is for $f \geq 891$ Hz, describe the zero-absorption data from ORCA very well. There are no ORCA data at a frequency sufficiently low to enable a comparison with rates determined by Equation (11) within the range $M \leq 1.886\left|g/g_t\right|^{1/3}/\left(1-g/g_t\right)^{1/6}$ for $f \leq 125$ Hz, however, the trend of the ORCA data is to "join the gap" between

the regions of the predicted curves for which data may be expected to be valid. The curve derived using the algorithm of Packman under-estimates ORCA data. As is described in more detail by Jones et al. (2015), the Packman algorithm assumes a ratio of sound speeds g/g_t equal to -1, and is not suitable for all situations.

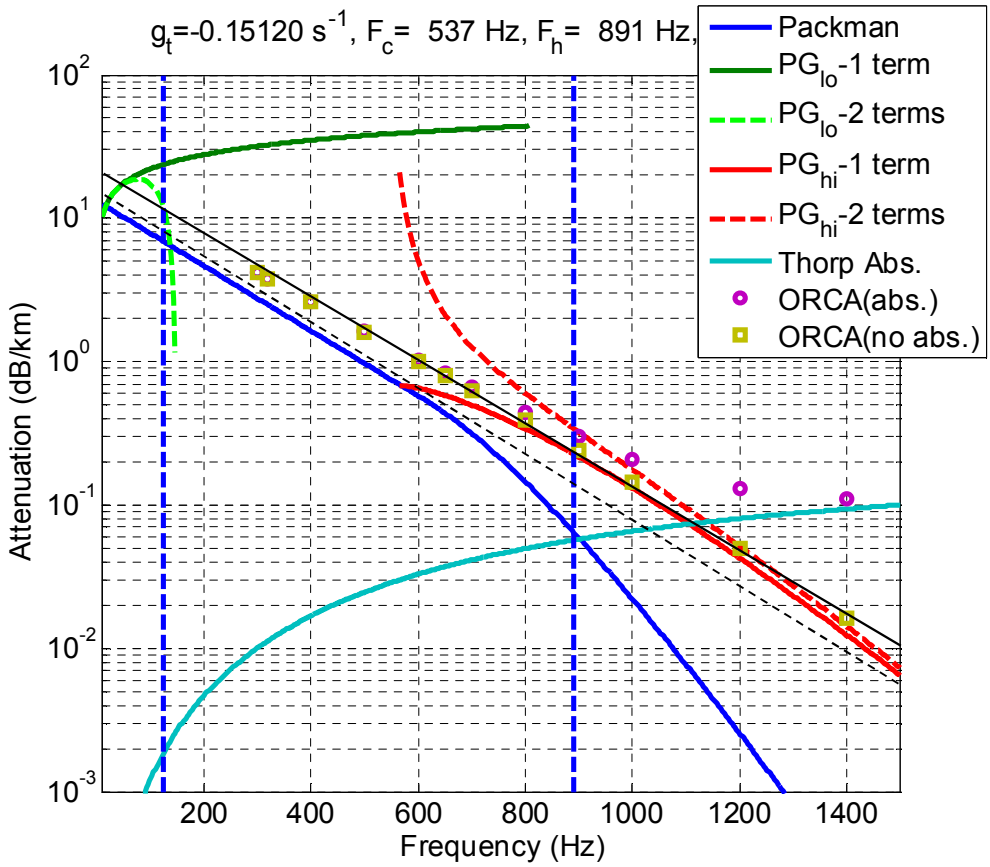

Figure 1: Leakage rate from 10 Hz to 1500 Hz for 1st mode for 50 m surface duct, $g/g_t = -0.1058$, vertical lines at frequencies 125 Hz and 891 Hz at which 2nd series terms in Equations (10) and (7) respectively are equal to half of 1st series terms, black line: tangent to Equation (8) data at 891 Hz, black dashed line: algorithm of Duan et al. (2016), blue line: algorithm of Packman (1990)

It is noteworthy that for frequencies less than about 891 Hz, at which $M < 2.3381 + \left([1 - g_t/g]/12\right)^{2/3}$, the ORCA data are very close to describing a straight line on the figure. Further, a straight line drawn to be a tangent to the curve from Equation (8) at 891 Hz very nearly passes through ORCA data at frequencies below 891 Hz. This suggests that over these frequencies the leakage rate $A_1(f)$ is of the form $K e^{-\eta f}$, where K and η are constants (obvious as $\log_{10}\left(K e^{-\eta f}\right) = \log_{10} K - \eta f[\log_{10}(e)]$). Considering Equations (3) and (8), for $M >> 2.3381$ $A_1(f)$ from Equation (8) will approximate the form $K e^{-\eta f}$, in which $\eta = \frac{4}{3}\pi (g)^{1/2}[1 - g/g_t](2D/c_w)^{3/2}$ with $\eta = 0.0097$ for the test scenario (but with K proportional to $f^{1/3}$ and varying slowly with f).

Significantly, ORCA data for scenarios otherwise identical but with values of below layer gradient g_t between $-0.05\,\text{s}^{-1}$ to -0.4 s^{-1} exhibited a good fit to the same tangent line drawn in Figure 1. This is exploited in section 4.

4. APPROXIMATION TO LEAKAGE RATE

For practical application, it is desirable to have a means to rapidly determine the rate of leakage from a mixed layer surface duct for different values of the magnitude of sound speed ratios $|g/g_t|$. From observation of the trend of the ORCA data in Figure 1, which follow an approximate straight line on the logarithmic plot for frequencies less than about 1000 Hz, it is conceivable that a semi-empirical algorithm may be prepared. Here, the

leakage rate would be taken from Equation (8) for frequencies greater than some nominal value f_n, but for lower frequencies would follow a tangent to the Equation (8) data at f_n.

Now Equation (8), which describes the leakage for frequencies above duct trapping, may be expressed as

$$A_1(f) \approx \frac{1406}{c_w}\left(\left[\pi f g^2\right]^{1/3}\right)\exp\left[-\tfrac{4}{3}(1-g/g_t)G(f)\right]\text{dB/km} \tag{13}$$

where the function $G(f)=(M-2.3381)^{3/2}$.

For frequencies less than the nominal value f_n, if the leakage expression takes the form

$$A_1(f)_{f<f_n} \approx \frac{1406}{c_w}\left(\left[\pi f_n g^2\right]^{1/3}\right)\exp\left[-\tfrac{4}{3}(1-g/g_t)\left[G(f_n)+(f-f_n)\left\{\left(\frac{d\,G(f)}{d\,f}\right)_{f=f_n}\right\}\right]\right]\text{dB/km} \tag{14}$$

the resultant leakage data $A_1(f)_{f<f_n}$ will follow a straight line on a plot of leakage rate vs frequency for which the leakage data are plotted on a logarithmic scale as in Figure 1. The data will also follow a tangent to the function for leakage $A_1(f)$ described by Equation (8) at frequency f_n.

Substituting for the dimensionless parameter *M* in terms of frequency *f* using Equation (3), it follows that

$$\frac{d\,G(f)}{d\,f}=\frac{M}{f}\left[M-2.3381\right]^{1/2} \tag{15}$$

where *M* has been re-substituted into the resulting expression. Hence Equation (14) may be written as

$$A_1(f)_{f<f_n} \approx \frac{1406}{c_w}\left[\pi f_n g^2\right]^{\frac{1}{3}}\exp\left[-\tfrac{4}{3}\left(1-\frac{g}{g_t}\right)\left[(M_n-2.3381)^{\frac{3}{2}}+\frac{(f-f_n)M_n}{f_n}\left[M_n-2.3381\right]^{\frac{1}{2}}\right]\right]\text{dB/km} \tag{16}$$

where M_n is the value of *M* at frequency f_n.

By eye, from Figure 1 it appears reasonable to select as f_n the frequency 890 Hz, as the tangent drawn from that point is a very good fit to the data for $f<890\,\text{Hz}$. It is just a coincidence that this frequency, which was originally considered as it corresponded with the second term in the square bracket in Equation (7) being 0.5, was a good starting point for the tangent line.

From Equation (7), it follows that

$$M_n=2.3381+\left(\left[1-g_t/g\right]/12\right)^{2/3} \tag{17}$$

and so $M_n-2.3381=\left(\left[1-g_t/g\right]/12\right)^{2/3}$, so that Equation (16) becomes

$$A_1(f)_{f<f_n} \approx \frac{1406}{c_w}\left(\left[\pi f_n g^2\right]^{1/3}\right)\exp\left\{-\frac{4}{3}\left(1-\frac{g}{g_t}\right)\left[\frac{1}{12}\left(1-\frac{g_t}{g}\right)+(f-f_n)\frac{M_n}{f_n}\left(\frac{1}{12}\left(1-\frac{g_t}{g}\right)\right)^{1/3}\right]\right\}$$

$$\approx \frac{1406}{c_w}\left(\left[\pi f_n g^2\right]^{1/3}\right)\exp\left\{-\frac{4}{3}\left(1-\frac{g}{g_t}\right)\left(\frac{1}{12}\left(1-\frac{g_t}{g}\right)\right)^{1/3}\left[\frac{f\,M_n}{f_n}+\left(\frac{1}{12}\left(1-\frac{g_t}{g}\right)\right)^{2/3}-M_n\right]\right\}\text{dB/km}. \tag{18}$$

Using Equation (17) to substitute for M_n gives

$$A_1(f)_{f<f_n} \approx \frac{1406}{c_w}\left(\left[\pi f_n g^2\right]^{\frac{1}{3}}\right)\exp\left\{-\frac{4}{3}\left(1-\frac{g}{g_t}\right)\left(\frac{1}{12}\left(1-\frac{g_t}{g}\right)\right)^{\frac{1}{3}}\left[\frac{f M_n}{f_n}-2.3381\right]\right\} \quad (19)$$

and so $A_1(f)_{f<f_n} \approx K e^{-\eta f}$ (20)

where $K = \frac{1406}{c_w}\left(\left[\pi f_n g^2\right]^{\frac{1}{3}}\right)\exp\left\{\frac{4\times 2.3381}{3}\left(1-\frac{g}{g_t}\right)\left(\frac{1}{12}\left(1-\frac{g_t}{g}\right)\right)^{\frac{1}{3}}\right\}$, (21)

and $\eta = \frac{4M_n}{3f_n}\left(1-\frac{g}{g_t}\right)\left(\frac{1}{12}\left(1-\frac{g_t}{g}\right)\right)^{1/3}$. (22)

Equations (20) through (22) may be seen to be in convenient form, as they are in terms of the in-layer and below-layer gradients g and g_t, the speed of sound at the surface c_w, the duct strength M_n, and the frequency f_n at which the function $K e^{-\eta f}$ is a tangent to the function for the leakage rate given by Equation (8). For the test case, by substituting appropriate values for the variables, it follows that $\eta = 0.00514$ and $K = 22.0$. The straight line drawn in Figure 1 adheres to this form. Equation (20) may be compared with the empirical expression for leakage obtained by Duan et al. (2016). This is unrelated to the below-layer gradient g_t, and is of the form

$$A_1(f) \approx 14.8\exp\left(-5.164\times 10^{-6}\, f\, D^{1.77}\right). \quad (23)$$

For the duct depth of 50 m, the expression is $A_1(f) \approx 14.8\exp(-0.00525 f)$, and is close to that expressed in Equations (20) to (22). From Figure 1, which shows the Duan et al. function, the agreement with ORCA data is not as good as for the leakage expression of Equations (20) to (22), but it is better than obtained with the Packman algorithm. It is interesting to see that, by substituting for M_n/f_n using Equation (3), from Equation (22) η becomes

$$\eta = \frac{4\pi}{3}\left(\frac{g}{M_n}\right)^{1/2}\left(\frac{2D}{c_w}\right)^{3/2}\left(1-\frac{g}{g_t}\right)\left(\frac{1}{12}\left(1-\frac{g_t}{g}\right)\right)^{1/3} \quad (24)$$

and a dependence on duct depth is introduced, although the exponent is 1.5, not 1.77 as in Equation (23).

4.1 Suggested algorithm for further testing

A comparison with data generated by ORCA for scenarios the same as the test case, but with values of below-layer gradient g_t ranging from $-0.05\,\mathrm{s}^{-1}$ to $-0.40\,\mathrm{s}^{-1}$, showed that leakage rates were relatively similar at corresponding frequencies, for frequencies below about 800 Hz. Further, for a leakage rate of the form $A_1(f)_{f<f_n} \approx K e^{-\eta f}$, it appeared that a good fit to all the leakage data was obtained when frequency f_n corresponded with M_n obtained by Equation (17) for the values of duct gradient $g = -0.016\,\mathrm{s}^{-1}$ and below-layer gradient $g_t = 0.1512\,\mathrm{s}^{-1}$, giving $\rho = -0.473$. A tentative suggestion is then that a candidate algorithm for further validation, and possible refinement, for different duct depths is:

- for frequencies $f \le f_n$, $A_1(f)$ is described by Equations (20) to (22) for $(g/g_t)^{1/3} = \rho = -0.473$, for M_n from Equation (17) being 3.250, and f_n being obtained from Equation (3) (and $f_n = 891$ Hz for a 50 m duct);
- for frequencies $f > f_n$, $A_1(f)$ is described by Equation (8) as evaluated for each case.

The leakage data for a scenario the same as the test case of Figure 1 but with a below-layer gradient g_t equal to $-0.05\,\mathrm{s}^{-1}$ are shown in Figure 2, and the corresponding data for a below-layer gradient of $-0.40\,\mathrm{s}^{-1}$ are shown in Figure 3. These figures show results that are typical of those obtained for various values of below-layer gradient

within the range $-0.05\,\mathrm{s}^{-1}$ to $-0.40\,\mathrm{s}^{-1}$, and may be considered to form a partial test of the candidate algorithm. For each figure, the leakage values obtained using the algorithms of Packman (1990) and Duan et al. (2016) are shown, and as these methods have no dependence on below-layer gradient, the respective functions are exactly the same as they are in Figure 1.

4.2 Discussion of simulated leakage data

In each of Figure 1, Figure 2 and Figure 3, for frequencies exceeding $f_n = 891\,\mathrm{Hz}$ the respective yellow ORCA data points for zero in-water absorption are very close to the curve described by Equation (8). Now, this function was derived from the first term in Furry's power series Equation (548) (Kerr, 1951) for application above the duct trapping frequency for the first mode $f_{c,1}$, and might be presumed to be appropriate only when the second term in the power series is insignificant. The right-most vertical blue dashed line in each figure marks the frequency at which the second term in Furry's power series is half the first term, yet for $f > 891\,\mathrm{Hz}$ the adherence of the ORCA data to each respective curve does not appear strongly related to the placement of the blue dashed line. Note that the absorption given by the Thorp expression, Equation (12), exceeds the leakage data at frequencies greater than about 1200 Hz. Hence, even though for each case Equation (8) well describes the leakage values over frequency $f_n = 891\,\mathrm{Hz}$, this is also somewhat irrelevant. The greater interest is in leakage data for lower frequencies.

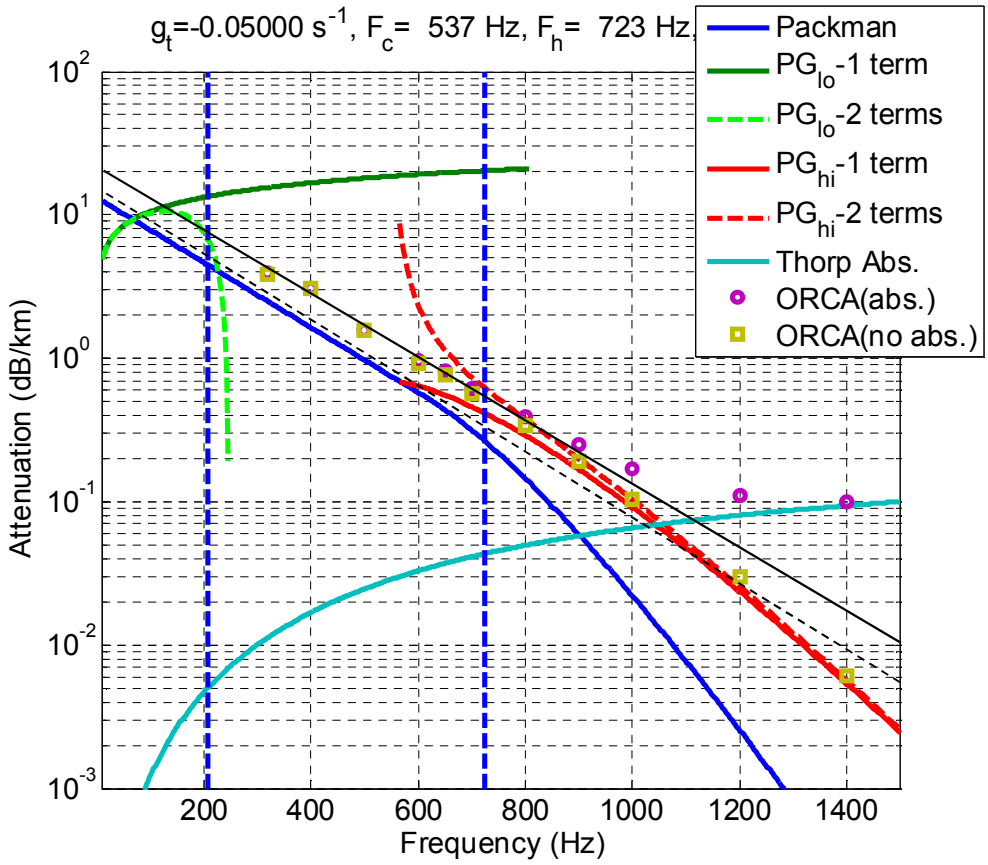

Figure 2. Leakage rate for 1st mode for 50 m surface duct, $g/g_t = -0.320$, vertical lines at frequencies at which 2nd series terms in Equations (10) and (7) are half of 1st series terms, black line: tangent to Equation (8) data at 891 Hz for $g/g_t = -0.1058$, black dashed line: algorithm of Duan et al. (2016), blue line: algorithm of Packman (1990)

For all datum points for frequencies below $f_n = 891\,\mathrm{Hz}$, for each of the values of below-layer gradient in the separate figures, the adherence to the straight line function $A_1(f) \approx 22.0\exp(-0.00514 f)$ described by Equations (20) to (22) is noteworthy. All relevant data in Figure 1 and Figure 2 are much closer to this line than to the lines obtained from the algorithms of Packman (1990) and Duan et al. (2016). In Figure 3, the ORCA data at the

lowest frequencies are slightly closer to the line from the algorithm of Duan et al., however, it may be argued that it is more important to describe the leakage near and slightly below the duct trapping frequency $f_{c,1}$, and the function $A_1(f) \approx 22.0 \exp(-0.00514 f)$ does that well.

Note that none of the ORCA values for each of the three cases was at a frequency sufficiently low to make a comparison with values of $A_1(f)$ determined by Equation (11). The simplified form of this expression shows a dependence on the below-layer gradient g_t, but no dependence on the duct gradient g. The expectation of increased leakage with a larger below layer gradient is not matched by the nearest datum points.

It is reasonable to now use the algorithm described in the previous section for a surface duct of depth 50 m for any value of below-layer gradient in the range $-0.05\,\mathrm{s}^{-1}$ to $-0.40\,\mathrm{s}^{-1}$. There will be a small disjoint in values at the frequency $f_n = 891\,\mathrm{Hz}$ at which the function for lower frequency differs from that for higher frequency, but this may be tolerated.

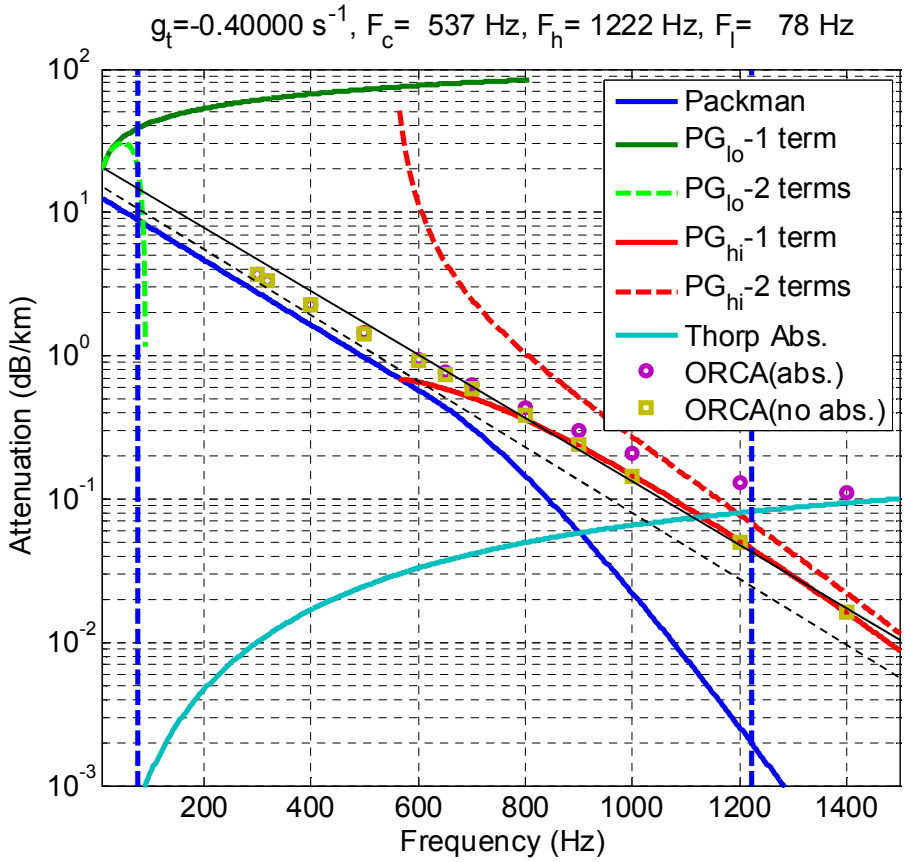

Figure 3. Leakage rate for 1st mode for 50 m surface duct, $g/g_t = -0.040$, vertical lines at frequencies at which 2nd series terms in Equations (10) and (7) are half of 1st series terms, black line: tangent to Equation (8) data at 891 Hz for $g/g_t = -0.1058$, black dashed line: algorithm of Duan et al. (2016), blue line: algorithm of Packman (1990)

4.3 Expected dependence on duct depth

In section 2, the leakage expression for frequencies above cut-on of the first mode is given in Equation (9) in terms of the duct trapping frequency $f_{c,1}$. This indicates that values of leakage determined from this expression will be the same so long as $f/f_{c,1}$ is the same. For example, if $f_{c,1}$ is larger by a factor X due to a decrease in duct depth D_{old} to D_{new}, it may be speculated that the entire leakage vs frequency plot retains the same shape if the frequency axis is such that $f/f_{c,1}$ values are retained in the same place. Now both Equation (9) and the "below duct trapping" expression (11) include a term in $f^{1/3}$, so if values of $f/f_{c,1}$ are retained in place on the plot, all

leakage vs frequency values will rise by $X^{1/3}$, and the slope of all portions of equivalent $f/f_{c,1}$ would be unchanged and unrelated to X. If the plot was then changed to have an absolute frequency scale, it follows that the slope of corresponding parts of equivalent $f/f_{c,1}$ scale with $1/X$. From Equation (1) it follows that the slopes also scale with $(D_{new}/D_{old})^{3/2}$. This may be seen as equivalent to the inclusion of the factor $D^{3/2}$ in the proposed relation for slope η in Equation (24).

It is, of course, speculation to suggest that these inferences from Equations (9) and (11) apply for values of frequency close to $f_{c,1}$, and an empirical determination of the dependence of the factor η on duct depth may still be needed.

5. CONCLUSIONS

The derivation of expressions, for the estimation of the coherent leakage rate for sound travelling underwater in a surface duct scenario, has been reviewed. With reference to simulated leakage data generated by a modal model for scenarios with a 50 m surface duct, a part-empirical algorithm for the determination of leakage has been proposed. The algorithm compares more favourably with leakage data generated by a modal model than alternative algorithms available in the literature. The feasibility of extending the algorithm for applications with surface ducts of different depth has been briefly considered.

REFERENCES

Ainslie, M.A. 2010, *Principles of Sonar Performance Modeling*, Springer

Duan, R.; Yang, K.; Ma, Y. and Chapman, N.R. 2016, *A simple expression for sound attenuation due to surface duct energy leakage in low-latitude oceans*, J. Acoust. Soc. Am. **139**, EL118

Jones, A.D.; Duncan, A.J. and Zhang, Z.Y. 2015, *Coherent Leakage of Sound from a Mixed Layer Surface Duct - Revisited*, Proceedings of Acoustics Hunter Valley, 15-18 November, Hunter Valley, Australia

Jones, A.D.; Duncan, A.J. and Zhang, Z.Y. 2016, *Practical Estimates of the Coherent Leakage of Sound from a Mixed Layer Surface Duct*, J. Acoust. Soc. Am. **139**, p. 2197

Kerr, D. E., ed. 1951, *Propagation of Short Radio Waves*, McGraw-Hill

Marsh, H. W. 1950, "Theory of the Anomalous Propagation of Acoustic Waves in the Ocean", *US Navy Underwater Sound Laboratory* USL Report No. 111, 12 May

Medwin, H. and Clay, C.S. 1998, *Fundamentals of Acoustical Oceanography*, Academic Press

Miller, J.C.P. 1946, "*The Airy Integral*", British Association Mathematical Tables, Cambridge

Packman, M.N. 1990, "A Review of Surface Duct Decay Constants", Proc. I.O.A., Vol. 12, Part 1, 139-146

Pederson, M.A. and Gordon, D.F. 1965, "Normal-Mode Theory Applied to Short-Range Propagation in an Underwater Acoustic Surface Duct", *Journal of the Acoustical Society of America*, **37**, 105-118

Pederson, M.A. and Gordon, D.F. 1970, "Theoretical Investigation of a Double Family of Normal Modes in an Underwater Acoustic Surface Duct", *Journal of the Acoustical Society of America*, **47**, 304-326

Porter, M.B. 2010, Acoustics Toolbox, Available from: http://oalib.hlsresearch.com

Urick, R.J. 1983, *Principles of Underwater Sound*, 3rd edition, Peninsula Publishing

Westwood, E.K., Tindle, C.T., and Chapman, N.R. 1996, "A normal mode model for acousto-elastic ocean environments", *J. Acoust. Soc. Am.,* vol. 100, pp. 3631-3645